ADVANCES IN ATMOSPHERIC SCIENCES, VOL. 21, NO. 6, 2004, 879–889

Simulation of Asian Monsoon Seasonal Variations with Climate Model R42L9/LASG

WANG Zaizhi*[1,2] (王在志), WU Guoxiong[1] (吴国雄), WU Tongwen[1] (吴统文), and YU Rucong[1] (宇如聪)

[1] *State Key Laboratory of Numerical Modeling for Atmospheric Sciences and Geophysical Fluid Dynamics, Institute of Atmospheric Physics, Chinese Academy of Sciences, Beijing* 100029

[2] *Guangzhou Institute of Tropical and Marine Meteorology, China Meteorological Administration, Guangzhou* 510080

(Received 22 December 2003; revised 31 May 2004)

ABSTRACT

The seasonal variations of the Asian monsoon were explored by applying the atmospheric general circulation model R42L9 that was developed recently at the State Key Laboratory of Numerical Modeling for Atmospheric Sciences and Geophysical Fluid Dynamics, Institute of Atmospheric Physics, Chinese Academy of Sciences (LASG/IAP/CAS). The 20-yr (1979–1998) simulation was done using the prescribed 20-yr monthly SST and sea-ice data as required by Atmospheric Model Intercomparison Project (AMIP) II in the model. The monthly precipitation and monsoon circulations were analyzed and compared with the observations to validate the model's performance in simulating the climatological mean and seasonal variations of the Asian monsoon. The results show that the model can capture the main features of the spatial distribution and the temporal evolution of precipitation in the Indian and East Asian monsoon areas. The model also reproduced the basic patterns of monsoon circulation. However, some biases exist in this model. The simulation of the heating over the Tibetan Plateau in summer was too strong. The overestimated heating caused a stronger East Asian monsoon and a weaker Indian monsoon than the observations. In the circulation fields, the South Asia high was stronger and located over the Tibetan Plateau. The western Pacific subtropical high was extended westward, which is in accordance with the observational results when the heating over the Tibetan Plateau is stronger. Consequently, the simulated rainfall around this area and in northwest China was heavier than in observations, but in the Indian monsoon area and west Pacific the rainfall was somewhat deficient.

Key words: Asian monsoon, simulation, seasonal variation, AMIP

1. Introduction

China experiences the influence of the Asian monsoon which has a significant impact on the regional and even the global climate. Asian monsoon research is always a hot topic. In earlier works, the Asian monsoon was only taken as the extension of the current Indian monsoon which belongs to the tropical monsoon. But later results (e.g., Tao and Chen, 1987) showed that the East Asian monsoon may be regarded as another subsystem differing from the Indian monsoon. As for the Indian monsoon system, the area-averaged precipitation can represent its strength and activity quite well. However, the East Asian monsoon is much more complicated. Up to now there is still no proper index to represent it. Further research has shown that the East Asian monsoon consists of tropical and subtropical monsoons, which are influenced by different synoptic systems (Zhu et al., 1987). Nevertheless, there is some interaction between the Indian and East Asian monsoons. In the order of onset, the Asian monsoon first breaks out in the South China Sea (SCS) and then extends northwestward (Tao and Chen, 1987). From the NCEP/NCAR (National Centers for Environmental Prediction/ National Center for Atmospheric Research) reanalysis data, Wu and Zhang (1998) pointed out that the onset of the Asian summer monsoon includes three sequential stages. The first stage is the onset over the eastern coast of the Bay of Bengal (BOB) in early May; then it breaks out over the SCS in middle May; and the last stage occurs over India in early June. According to these results, the onset of the East

*E-mail: zaizwang@mail.iap.ac.cn

Asian Monsoon is about one month earlier than the Indian monsoon. The strength of the two monsoons are negatively correlated, which means that when the East Asian monsoon is strong, the Indian one is weak, and vice versa.

GCMs are a very useful tool to understand the Asian monsoon climate and its variations. Many GCM results (Hoskins and Rodwell, 1995; Liu and Wu, 1997; Fu et al., 2002; Kang et al., 2002) have shown that the basic distribution of monsoon circulations such as the subtropical high, the equatorial jets, the monsoon low, etc. can be reproduced quite well, but their strengths and variations are hard to simulate well. Precipitation is even harder to successfully simulate by GCMs (Kang et al., 2002). A wide range of skill exists among GCMs in simulating monsoon precipitation, which is largely attributed to the different sub-gridscale parameterization schemes and horizontal resolutions in the GCMs (Sperber et al., 1994). Generally, a GCM with higher horizontal resolution is able to capture smaller scale features of the circulation and precipitation.

The monsoons are known to be the result of the land-sea thermal contrast (Kuo and Qian, 1982). Besides the massive Asian continent, the Tibetan Plateau, which averages over 4000 m in height, plays an important role in the onset, strength and evolution of the Asian monsoon (Hahn and Manabe, 1975). Fennessy et al. (1994) found the simulated India monsoon rainfall with a mean orography is better than an enhanced silhouette orography. Hoskins and Rodwell (1995) investigated the effects of mountains, diabatic heating, and nonlinear interactions on the Asian summer monsoon. A linear version of their model forced with diabatic heating without mountains is able to reproduce the upper-tropospheric circulation. Mountains and nonlinear interactions are essential to realistically simulate low-level monsoon inflow. Atmosphere-ocean coupling also plays a critical role in simulating the realistic mean state of the Asian summer monsoon and intraseasonal oscillation (Fu et al., 2002). Air-land interaction has a comparable influence on the mean climate and seasonal variations of the Asian monsoon (Liu and Wu, 1997). Yang and Lau (1998) examined the relative importance of SST and ground wetness (GW) in the variability of the monsoon. They showed that ocean basin-scale SST anomalies exert a stronger control on the interannual variability of the monsoon than GW anomalies. Wang and Qian (1997) discussed the influences of the diurnal variation of the solar radiation and found that it does not influence the mean monsoon system in the quasi-equilibrium state, but it does influence its intensity and the precipitation pattern significantly.

The simulated monsoon is also sensitive to a model's horizontal resolution. Generally, with respect to large-scale features of the circulation, the largest differences among the simulations occur at T42 relative to T21. Higher resolutions than T42 such as T106 can better capture both the spatial and temporal characteristics of the Indian and East Asian monsoons (Sperber et al., 1994). Regional climate models (RegCM) with even higher resolution have been developed to simulate summertime climate over East Asia (Liu et al., 1994; Wang et al., 2003).

In the present study, the atmospheric general circulation model (R42L9) recently improved at the State Key Laboratory of Numerical Modeling for Atmospheric Sciences and Geophysical Fluid Dynamics, Institute of Atmospheric Physics, Chinese Academy of Sciences (LASG/IAP/CAS) is utilized to simulate the Asian monsoon, focusing on the features of the climatological mean, seasonal variations, and the interannual variations. Section 2 describes the model and observational data used in the present study. The climatology and seasonal variations of the Asian monsoon are presented in section 3. Section 4 presents conclusions and discussions.

2. The model and observational data

The rhomboidally truncated spectral model (R15L9) of Bourke (1974) was introduced to LASG/IAP/CAS in 1991. Some important developments were made afterwards. The 'standard atmosphere' concept was introduced to the model by subtracting a standard atmospheric profile of temperature and pressure to reduce errors. A K-distribution radiation scheme (Shi, 1981), Slingo's cloud diagnosis scheme (Slingo, 1987), the diurnal variation of solar radiation (Shao et al., 1998), and the simplified simple biosphere model (SSiB) (Xue et al., 1991; Liu and Wu, 1997) were also adopted. In addition, the model was successfully coupled with the LASG ocean GCM to form a coupled global ocean-atmosphere-land system (GOALS), which is able to simulate interannual and interdecadal climate variability (Guo et al., 2000; IPCC, 2001). The model details can be found in Zhang et al. (2000), Wu et al. (1996, 1997), and Wu et al. (2003). Despite the general success of the model simulation, there are some deficiencies mainly due to its coarse resolution, especially in Asia where the orography is complex and the air-land-sea interaction is very important.

The model was recently upgraded from R15 to R42. Its horizontal resolution was raised from 7.5° (lon)×4.5° (lat) to 2.8125° (lon)×1.66° (lat). The related forcing data such as topography, land-sea distri-

bution, vegetable types, etc. were also updated. The radiation process which uses most of the computing cycles in R42L9 was parallelized with the Open Specifications for Multi Processing (OpenMP) method. The program was also standardized for further development. The model performance was then evaluated and compared with the original R15L9/LASG model by Wu et al. (2003) by simulating mainly the global climatological mean states. They showed that the R42L9 model well reproduces the observed basic patterns and significantly improves the simulation compared to the original R15L9/LASG model.

In this paper, the model runs for 20 model years following the AMIP II requirement from 1979 to 1998 using the observed monthly SSTs and sea ice data provided by the Program for Climate Model Diagnosis and Intercomparison (PCMDI) to validate its regional performance. The seasonal variations of the Asian monsoon, mainly the precipitation and related circulations, are assessed to evaluate the model's ability to simulate the Asian monsoon. The 20-yr (1979–98) NCEP/NCAR reanalysis (Kalnay et al., 1996), the Climate Prediction Center (CPC) merged precipitation data (CMAP) (Xie and Arkin, 1996), and the CPC monthly OLR are used for comparison.

3. Results

3.1 *Precipitation*

Figure 1 shows the June-July-August (JJA) mean precipitation from the simulation and observations. Compared to CMAP precipitation (Fig. 1b), the model has captured maximum centers on the west coast of India, over BOB, and in the ITCZ along the equator. The belt of large precipitation over the southern Indian Ocean in the model is also similar to the observed. The observed minimum precipitation off the southeast coast of India is obvious in the simulation. We also note that the observational rainband in East

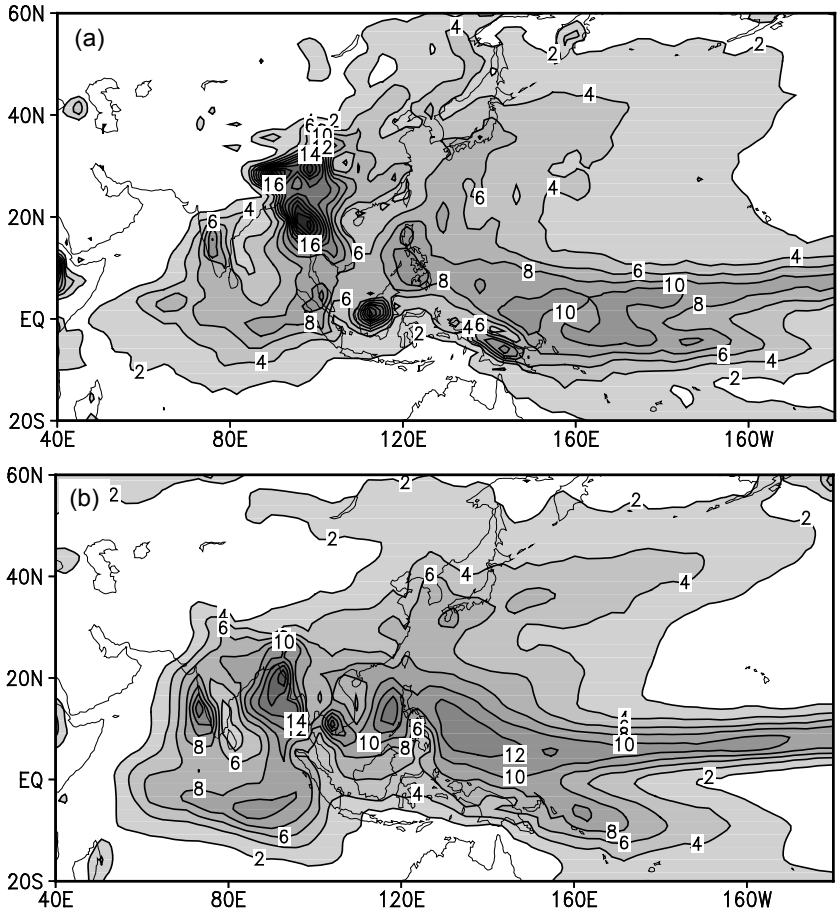

Fig. 1. Mean JJA precipitation (mm d^{-1}) from (a) the model simulation; (b) CMAP. Contour interval is 2 mm d^{-1}. The shading indicates a rainfall rate of more than 2 mm d^{-1}.

Asia, which extends to the middle Pacific, has been reproduced. In many GCMs presented by Kang et al. (2002), this rainband was poorly simulated and distributed in the landward side of East Asia. Precipitation is the main representation of a monsoon, and in the model, it is the composite result of the dynamics and physical processes. From this point of view, the model can simulate the mean Asian summer monsoon quite well. However, there are some regional differences between the simulation and observation. The maximum centers over India and the West Pacific are weaker, while the center over the BOB is much stronger than the CMAP. The location of the maximum over the west Pacific is shifted eastward. The South Pacific Convergence Zone (SPCZ) precipitation, also, is not well represented. This implies that the simulated monsoon strength is not very good. After analyzing 10 GCMs participating in the AMIP, Kang et al. (2002) pointed out that there is one category of models (including R15L9/IAP) in which the simulated precipitation is confined near the equatorial region and in which less precipitation occurs in the subtropical West Pacific compared to the observation. They suggested that the deficiencies were related to the physical parameterizations, particularly for the convection. Now although, the horizontal resolution of the current model version increases from R15 to R42, the physical parameterization schemes remain the same. So the model biases in R15L9 and R42L9 are similar. Another possible reason for the regional differences may come from an improper description of the maritime continent. The maritime continent, with islands and shallow seas, is a major challenge to models which tend to systematically underestimate the precipitation in this region. Neale and Slingo (2003) showed that the deficient rainfall over the Maritime Continent could be a driver for other systematic errors through the circulation and influence to the global circulation. Figure 1a also shows some unrealistic centers such as the maximum center over the southeastern Tibetan Plateau and two centers over the Indonesian area that also appeared in other models (Yu et al., 2000). These may be caused by the Gibbs error associated with the truncation of local orography or the improper vegetation distribution over the land.

The Asian monsoon consists of two components, the South Asian or Indian monsoon and the East Asian monsoon (Tao and Chen, 1987). Both have distinct evolutionary features. The time-latitude sections of precipitation averaged over the longitudes of 60°–105°E and 105°–120°E are shown in Figs. 2 and 3, respectively. They present seasonal evolutions of the Indian monsoon and the Eastern Asian monsoon. As shown in Fig. 2b, the Indian summer precipitation from CMAP is mainly centralized from May to September. In early June, the large precipitation is located at 10°N, with the maximum center of 10 mm d^{-1}. Then it extends northward with time. In the middle of July, it moves to about 20°N. This feature of the timing has been simulated in the model as shown by the arrows in Fig. 2a, though the amount of precipitation is slightly smaller than in CMAP, and the center in early June is not so clear. In Fig. 2, the large model biases occur near 27°N where there is a maximum precipitation from the R42L9 model almost all year round, but this is not seen in CMAP. Since this latitude is just located to the south of the Tibetan Plateau, the simulated biases may be caused by the local topography, because the thermal and dynamic effects of the Tibetan Plateau have a vital impact on the monsoon circulation and precipitation (Liu, 2000). Figure 3b shows the evolution of the East Asian monsoon precipitation. A rainfall belt between 20° and 30°N before May is commonly called the spring persistent rains (SPR) over central China, and it moves slightly southward with time because of the winter monsoon activities in this area. In June, the rainband moves northward due to the onset of the SCS monsoon. There is a maximum belt around 30°N, which is proximately correspondent to the mei-yu rainfall zone. The belt extends further northward to North China in July. From June on, there is another belt of maximum rain in the SCS, which represents the ITCZ. The above steps are typical in East Asia. Figure 3a shows that these steps can be reproduced as the arrows show, though the precipitation before May is too large and the rain belt is somewhat shifted northward. Also, the simulated ITCZ is weaker, and the rain belt is sustained in the north and retreats more slowly in autumn as observed.

Figures 4a–b show the annual cycle of area-averaged precipitation over the Indian monsoon (5°–30°N, 60°–105°E) and East Asian monsoon (22.5°–45°N, 105°–140°E) domains, respectively. It is clear that the seasonal evolutions of precipitation in both the Indian and East Asian monsoon areas are approximately coincident with those from the CMAP data. In the East Asian monsoon area, the observed increase from January to June (Fig. 4a) and the later decrease are simulated realistically, and in the Indian monsoon area, the sudden increase in May and sustained level from June to August are simulated. However, there are some differences between the simulation and observation. For example, the precipitation in East Asia is larger, which suggests that the modeled East Asian monsoon is stronger than the observation. The simulated precipitation in the Indian monsoon area is less

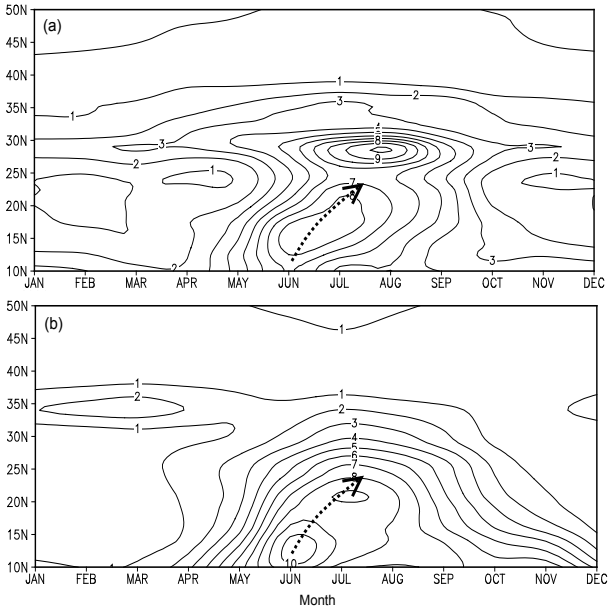

Fig. 2. Time-latitude sections of zonal averaged precipitation (mm d^{-1}) along 10°–50°N over the Indian monsoon area (60°–105°E) from (a) the model simulation; (b) CMAP. The arrows denote the main precipitation stages. Contour interval is 1 mm d^{-1}.

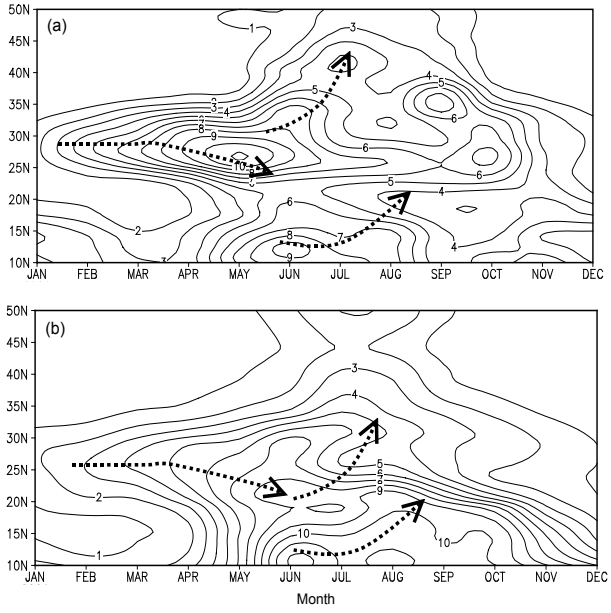

Fig. 3. As in Fig. 2 except over the East Asian monsoon area (105°–120°E mean).

than that of CMAP from May to September, which reflects that the simulated Indian summer monsoon is weak.

In Fig. 4a, there is another peak due to the ITCZ in August, which is not obvious in the simulation. This implies that the simulated East Asian monsoon circulation in August is unrealistically displaced southward,

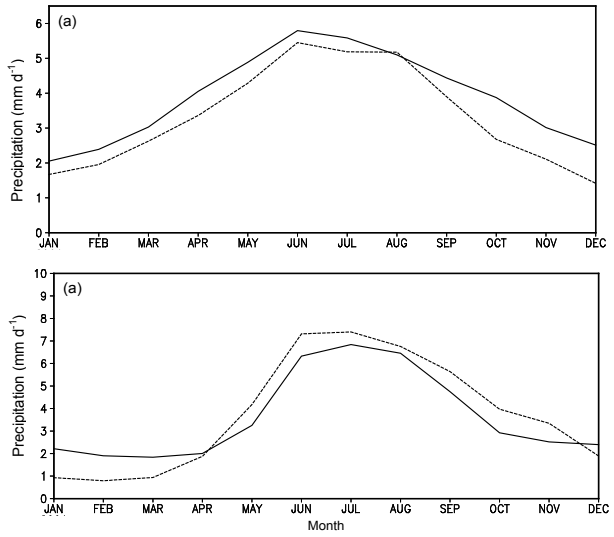

Fig. 4. Annual cycle of area averaged precipitation (mm d^{-1}) over (a) East Asian monsoon area (22.5°–45°N, 105°–140°E,), and (b) Indian monsoon area (5°–30°N, 60°–105°E). The solid line is from the simulation and the dashed is from CMAP.

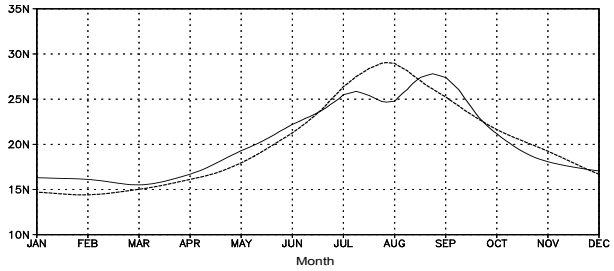

Fig. 5. Climatological timing of 500 hPa ridge, represented by the mean latitudes where the zonal wind is zero, from 110°–140°E. The solid line is from the simulation and the dashed is from the NCEP/NCAR reanalysis.

which causes the rain belt to be sustained in North China and the somewhat weak precipitation over the SCS. Figure 5 displays the latitudes of the monthly western Pacific subtropical high ridgeline, i.e., the mean latitude of zero zonal wind averaged from 110°–140°E. The time evolution from the R42L9 simulation is in accordance with that from the NCEP reanalysis data except in August when the NCEP's mean ridge spreads to about 29°N and reaches its northmost position, while the simulated western Pacific subtropical high moves unrealistically from north to south. This leads to a weak ITCZ and a strong East Asian monsoon in the model.

3.2 *Asian monsoon circulations*

In section 3.1, the simulated spatial and temporal distributions of precipitation are evaluated using the

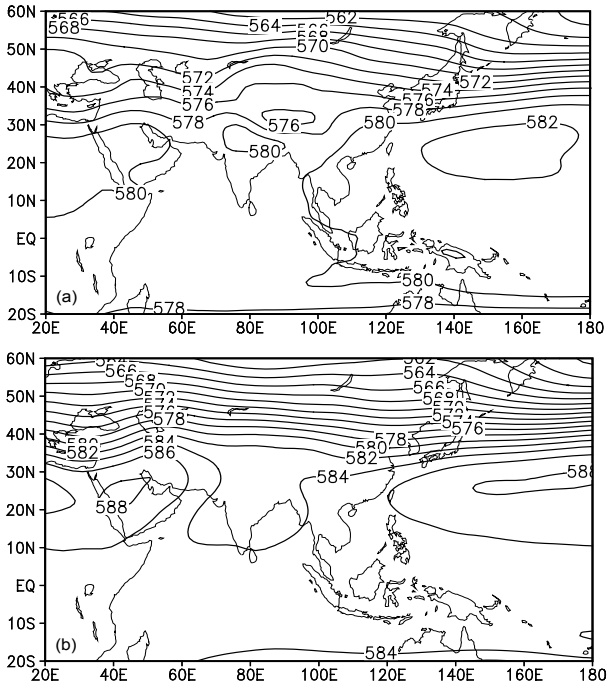

Fig. 6. Mean JJA 500 hPa height (gpdm) from (a) the model simulation; (b) NCEP/NCAR reanalysis. Contour interval is 2 gpdm.

observational data. Though the model can simulate observational patterns quite well, there are some deficiencies, especially in the monsoon strengths and the rainfall around the Tibetan Plateau. In this section, the circulation, which is another important aspect to represent the monsoon, is evaluated with the observations, as well as its relations to monsoon precipitation.

3.2.1 500 hPa *height*

Figure 6 shows is the mean 500 hPa height field in JJA. The main features can be simulated quite well, such as the Iran high and the western Pacific subtropical high, as well as the Indian monsoon low between these two highs. The amplitude is somewhat lower than the observations, especially in the Tropics. The bias is about 6 gpdm. This bias also exists in R15L9 and in R42L9 evaluated by Wu et al. (2003). The authors supposed that it is due to the underestimation of low level clouds. So in this version, the observed International Satellite Cloud Climatology Project (ISCCP) total cloud is introduced into the model to replace the diagnosed cloud. However, the improvement is not as significant as expected. This indicates that other processes, such as the convective and boundary-layer parameterizations, should be improved. There are some differences between the simulation and NCEP/NCAR reanalysis. The Indian monsoon low is confined to the Tibetan Plateau, which is consistent with the lower precipitation in the Indian area, and more precipitation over the plateau. The ridge of the western Pacific subtropical high is shifted southward compared to the observation, as shown in Fig. 5. The relationship between the subtropical high and rainfall is complicated. According to thermal adaptation theory (Wu and Liu, 2000; Liu et al., 1999), the condensation heating plays an important role in the formation and location of the western Pacific subtropical high. From Fig. 1a, it can be seen that the simulated precipitation over the BOB is stronger and that the center is over the southeast Tibetan Plateau indicating that the condensation heating over this area is larger. According to observational study (Liu, 2000), strong heating over the Tibetan Plateau can stimulate a Rossby wave train on the east coast of Asia that induces an anticyclonic anomaly south of 30°N and a cyclonic anomaly north of 30°N in the West Pacific. This may lead to the southward shift of the subtropical high from about 30°N to 25°N as shown in Fig. 5.

3.2.2 *Mean sea level pressure* (*MSLP*)

Figures 7a and 7b display the simulated and observed JJA MSLP respectively. Comparing these two fields, we can see that the main features of the monsoon systems are similar, such as the Indian monsoon low, the western Pacific subtropical high, and the Siberian high. The differences are also obvious. A low is located

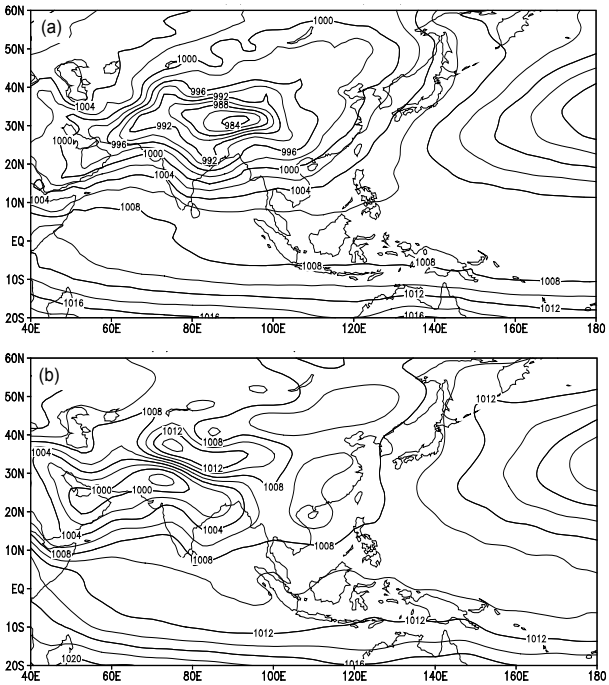

Fig. 7. Mean JJA sea level pressure (hPa) from (a) the model simulation; (b) NCEP/NCAR reanalysis. Contour interval is 2 hPa.

over the Tibetan Plateau in the simulation, while a high dominates this area in the observation. This low indicates that the simulated heating is stronger over this area as discussed in section 3.1. It may also be partly due to the inconsistent post-processing scheme used to compute the MSLP. The simulated Indian monsoon is weak, which is consistent with the previous analysis of precipitation. The Siberian high ridge in the observation is weakly simulated by the model, which may cause the northward shift of the precipitation in North China. The western Pacific subtropical high is about 2 hPa weaker than the observation and the extension of the ridge toward to Japan is not simulated.

3.2.3 *Outgoing longwave radiation* (*OLR*)

Since OLR can represent convective activity in the Tropics, we show its distribution in Fig. 8. The lightly shaded area denotes values less than 230 W m^{-2}, and the heavily shaded area denotes values less than 210 W m^{-2}. In the Tropics, the 230 W m^{-2} contour is distributed in a very similar way to the observed over the West Pacific, BOB and Indian area, which shows that the model simulates the monsoon quite well. The missing region of 210 W m^{-2}, which is consistent with the lower rainfall in the West Pacific, shows that the deep convection needs to be improved. Other studies have shown that the convective process in the West Pacific area is very important for simulating the East Asian monsoon. In the North Pacific, the simulated OLR is lower than the observations. Since OLR here does not represent convection but surface temperature under a clear sky, which is prescribed as the SST in this simulation, the radiation process may influence this low center, or the cloud top is high as Wu et al (2003) pointed out.

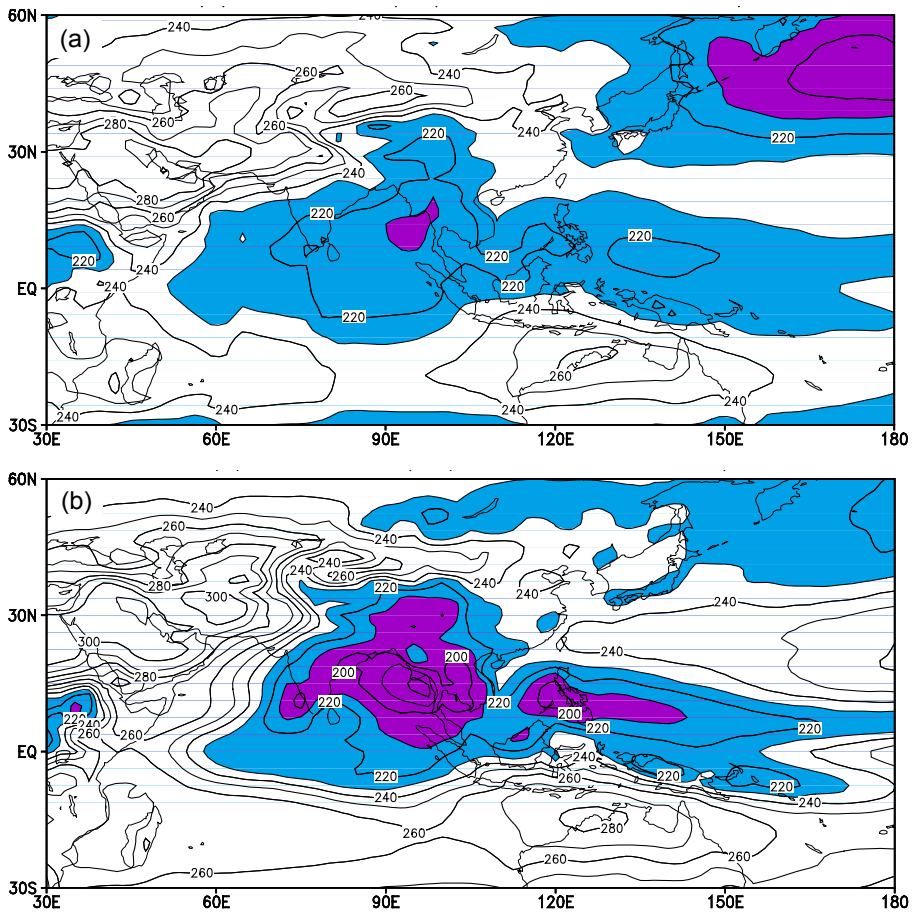

Fig. 8. Mean JJA OLR (W m^{-2}) from (a) the model simulation; (b) NCAR. Contour interval is 10 W m^{-2}. Light and heavy shadings indicate the OLR less than 230 W m^{-2} and 210 W m^{-2}, respectively.

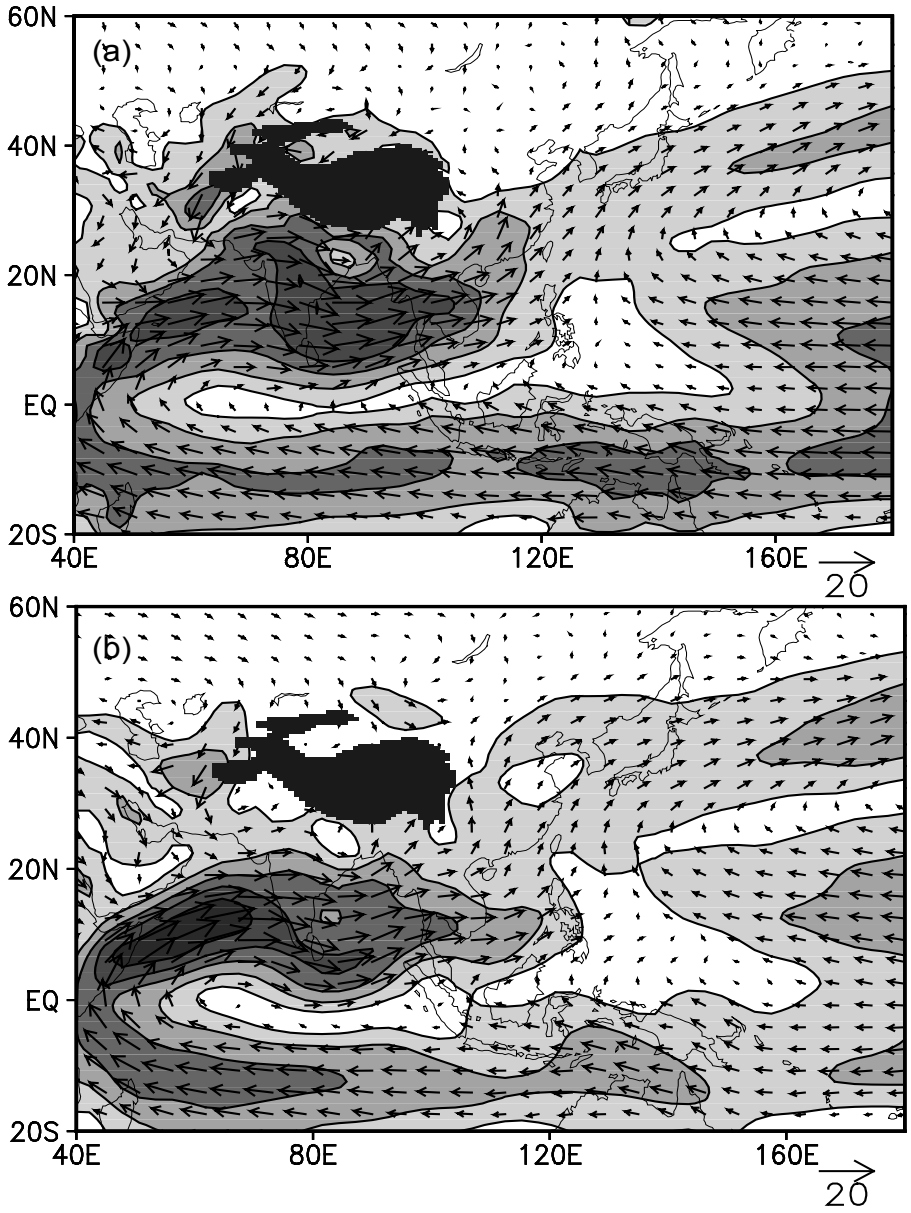

Fig. 9. Mean JJA 850 hPa wind (m s^{-1}) from (a) the model simulation; (b) NCEP/NCAR reanalysis. Contour interval is 5 m s^{-1}.

3.2.4 *Wind*

Now the wind fields at 850 hPa and 200 hPa are compared in this sub-section. Monthly results (not shown) show that the monsoon system patterns and time evolutions can be simulated properly in this model. Figure 9 shows the 850 hPa JJA mean wind, with the shading indicating wind speeds more than 5 m s^{-1}. The main features shown in the observations (Fig. 9b), such as the Somalian equatorial jet, the southwesterly over the Indian Ocean and its extension to East Asia, and the cross-equatorial jet over 105°E, can be captured properly. And the southwest stream in the west part of the western Pacific subtropical high is simulated well. The area where wind speed exceeds 5 m s^{-1} is very similar to that in Fig. 9a. The low level monsoon circulation is reproduced in the model.

The most obvious difference between the simulation and the observed is over the Arabian Sea, where the westerly is about 4 m s^{-1} stronger than the NCEP reanalysis. This strong westerly extends not eastward to the SCS as in the observations, but northeastward to dominate East Asia, including South and East

China. This indicates that the East Asian monsoon is stronger in the model, which agrees with previous precipitation results. Over the south part of the SCS where the westerly dominates in the observation (Fig. 9b), the simulated wind is weaker due to its northward extension to China. The wind over South China is stronger and converged to southwest China. The precipitation in the Yangtze River valley and North China is larger while the precipitation over the SCS is smaller. We also note that the trade wind in Indonesia is stronger in the model, which may be related to the SPCZ deficiency.

At 200 hPa (figure omitted), the establishment and evolution of the South Asian high from spring to summer is clear and accords with the NCEP reanalysis data. The westerlies are weaker approximately along 35°N, while the easterlies in the Tropics are too strong in summer. The South Asian high center is mainly located over the Tibetan Plateau area, which shows the east or Tibetan pattern shown by Zhang et al. (2002).

The wind shear between 850 hPa and 200 hPa averaged over the region of 0°–20°N, 40°–110°E is usually defined as an Asian summer monsoon index (WYI) (Webster and Yang, 1992). Figure 10 shows the area-averaged wind at 850 and 200 hPa and the computed monsoon index. Though the simulated Somalia jet is weak, the wind over the Arabian Sea is strong at 850 hPa (Fig. 9a). The area mean is similar and the two curves in summer time at 850 hPa are almost the same in Fig. 10a. However, the simulated easterly is stronger than the observations throughout the whole year at 200 hPa. The simulated WYI shown in Fig. 10b is larger, and the onset of the Asian summer monsoon in the model is earlier than in the observations. Though the monsoon index is sensitive to the region which is chosen for calculating the index, the WYI is consistent with the heating simulated over the Tibetan Plateau shown in previous sections. The heating is strong in the simulation, which causes high temperature over the Tibetan Plateau and a greater temperature gradient. As the vertical wind shear is related to the temperature latitude gradient, the greater heating over the Tibetan Plateau may cause the larger WYI.

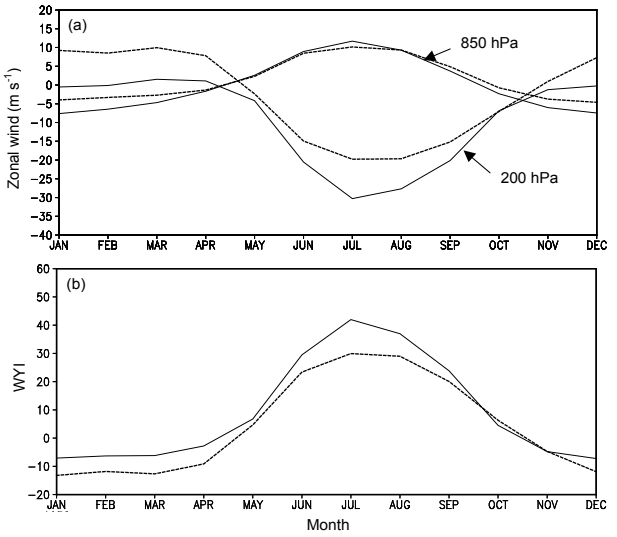

Fig. 10. Time series of (a) area mean zonal wind ($\mathrm{m\,s^{-1}}$) at 850 hPa and 200 hPa; (b) the WYI. The area is 5°–20°N, 40°–110°E, and the solid and dashed lines denote the simulation and NCEP/NCAR reanalysis, respectively.

4. Summary

In this study, the performance of the model AGCM R42L9/LASG is assessed in simulating the mean and seasonal variability of the Asian monsoon. Through the comparison between the simulated precipitation and the CMAP data, the main features of the geographical distribution and seasonal variations can be properly captured. The centers over India and the BOB in summer are simulated successfully. The rainband from East China to the Northwest Pacific is also reproduced. Since the simulation of precipitation over Asia is very difficult, and since few models can simulate the distribution correctly from the AMIP results, this model has improved quite significantly. The time evolution is simulated both over India and East Asia. However, there are also some deficiencies, especially over the Tibetan Plateau and the tropical West Pacific. Over the Tibetan Plateau, the rainfall is overestimated compared with the observations, and the heating is stronger. This deficiency may be due to the complex terrain and vegetation. Though the topography is interpolated from very high resolution data ($10' \times 10'$), it is still not fine enough to represent the vegetation distribution and the hydrological process. Consequently, the Indian monsoon low is weaker, and the strength of the Indian monsoon is also weaker compared to the observations. Meanwhile, the strength of the East Asian monsoon is stronger due to the localization of the monsoon low at low levels and the South Asian high at high levels over the Tibetan Plateau area. The underestimated precipitation over the tropical West Pacific may be due to the convective parameterization as shown from the OLR comparison. To improve the ability of the Asian monsoon simulation, the physical processes, especially the topography and convective parameterization, are our main emphases in the future. In addition, the vertical resolution should also be increased to describe the physical processes properly.

We also note that the differences here do not mean that the simulation is totally wrong, as the precipitation is a very difficult field to observe and thus one should be cautious in using it for evaluation purposes. The CMAP dataset uses several estimates of precipitation as measured by satellite over land and oceans, as well as the rain gauge data over land. The rain gauge observation is scarce and local, while the cloud features are special around the Tibetan Plateau area. The precipitation quality is doubtful. The CMAP data utilized in this paper is $2.5^\circ \times 2.5^\circ$, which may represent the rainfall consistent with this scale. The model resolution in the meridional direction is about 1.66° and is higher than the observations, so some small scale processes related to the orography may not be simulated. From the rain gauge observations we know that some in situ precipitations are very strong on the east periphery of the Tibetan Plateau due to the topographic convergence (Yu et al., 2000). The model may respond to this mechanical forcing but with effects exaggerated somehow.

The circulation fields, such as 500 hPa height, MSLP and wind at 850 and 200 hPa, are compared with the observations. Results show that the model is able to reproduce the main features such as the subtropical high, the monsoon low, the equatorial jets and the southwesterlies etc. over the monsoon area. From the temporal comparison, the model can simulate the monsoon onset and evolutions properly before August. Some deficiencies are due to the heating over the Tibetan Plateau. The western Pacific subtropical high is displaced southward compared to the observation, which is consistent with the rain distribution. The strong heating over the Tibetan Plateau produces a large WYI and a strong mean Asian monsoon.

The deficiencies in our model are common in other climate models as the AMPI results show (Yu et al., 2000; Kang et al., 2002). Some common processes may be missed in the AMIP-like simulation. For example, the SSTs and sea ice are prescribed, so that the atmosphere is passive and has no influence on the ocean circulation. In the Tropics, the air-sea interaction plays a very important role in the seasonal and interseasonal variations, which also has a great influence on the global climate. Coupling this model properly with an ocean model is an important task to improve the simulations in the future.

Acknowledgments. We would like to thank NCAR for access to Xie and Arkin's rainfall data archives and for providing the NCEP/NCAR reanalysis data. This work was conducted under the joint support of Chinese Academy Project ZKCX2-SW-210 and the National Natural Science National Foundation of China under Grant Nos. 40231004, 40135020, 40221503, 40233031, and 40475027.

REFERENCES

Bourke, W., 1974: A multi-level spectral model. I. Formulation and hemispheric integrations. *Mon. Wea. Rev.*, **102**, 687–701.

Fennessy, M. J., and Coauthors, 1994: The simulated Indian monsoon: A GCM sensitivity study. *J. Climate*, **7**, 33–43.

Fu, X., B. Wang, and T. Li, 2002: Impacts of air-sea coupling on the simulation of mean Asian summer monsoon in the ECHAM4 model. *Mon. Wea. Rev.*, **130**, 2889–2904.

Guo Yufu, Yu Yongqiang, and Zhang Tao, 2000: Evaluation of IAP/LASG GOALS model. *IAP Global Ocean-Atmosphere-Land System Model*. Zhang et al., Eds., Science Press, Beijing, 252pp.

Hahn, D. G., and S. Manabe, 1975: The role of mountains in the South Asian monsoon circulation. *J. Atmos. Sci.*, **32**, 1515–1541.

Hoskins, B. J., and M. J. Rodwell, 1995: A model of the Asian summer monsoon. Part I: The global scale. *J. Atmos. Sci.*, **52**, 1329–1340.

IPCC, 2001: *Climate Change 2001, The Scientific Basis*. Contribution of working Group I to the Third Assessment Report of the Inter-governmental Panel on Climate Change (IPCC). Houghton et al., Eds., Cambidge University Press, 892pp.

Kalnay, E., and Coauthors, 1996: The NCEP/NCAR 40-year reanalysis project. *Bull. Amer. Meteor. Soc.*, **77**, 437–471.

Kang, I. S., and Coauthors, 2002: Intercomparison of the climatological variations of Asian summer monsoon precipitation simulated by 10 GCMs. *Climate Dyn.*, **19**, 383–395.

Kuo, H. L., and Y. Qian, 1982: Numerical simulation of the development of mean monsoon circulation in July. *Mon. Wea. Rev.*, **110**, 1879–1897.

Liu Hui, and Wu Guoxiong, 1997: Impacts of land surface on climate of July and onset of summer monsoon: A study with an AGCM plus SSiB. *Adv. Atmos. Sci.*, **14**, 289–308.

Liu Xin, 2000: Impacts of the diabatic heating over the Tibetan Plateau on the Asian atmospheric circulation. Ph. D. dissertation, Institute of Atmospheric Physics, IAP, 106pp. (in Chinese)

Liu Yiming, Wu Guoxiong, Liu Hui, and Liu Ping, 1999: The effect of spatially nonuniform heating on the formation and variation of subtropical high. Part III: Condensation heating and South Asia high and western Pacific subtropical high. *Acta Meterologica Sinica*, **57**, 525–538. (in Chinese)

Liu, Y. Q., F. Giorgi, and W. M. Washington, 1994: Simulation of summer monsoon climate over East Asia with an NCAR regional climate model. *Mon. Wea. Rev.*, **122**, 2331–2348.

Neale, R., and J. Slingo, 2003: The maritime continent and its role in the global climate: A GCM study. *J. Climate*, **16**, 834–848.

Shao, Hui, Qian Yongfu, and Wang Qianqian, 1998: The effects of the diurnal variation of solar radiation on climate modeling of R15L9. *Plateau Meteorology.*, **17**, 158–169. (in Chinese)

Shi Guangyu, 1981: An accurate calculation and representation of the infrared transmission function of the atmospheric constitutes. Ph. D. dissertation, Tohoku University of Japan, 191pp.

Slingo, J. M., 1987: The development and verification of a cloud prediction scheme for the ECMWF model. *Quart. J. Roy. Meteor. Soc.*, **113**, 899–927.

Sperber, K. R., S. Hameed, G. L. Potter, and J. S. Boyle, 1994: Simulation of the northern summer monsoon in the ECMWF model: Sensitivity to horizontal resolution. *Mon. Wea. Rev.*, **122**, 2461–2481.

Tao Shiyan, and Chen Longxun, 1987: A review of recent research on the East Asian summer monsoon in China. *Monsoon Meteorology*, C.-P. Chang and T. N. Krishnamurti, Eds., Oxford University Press, 60–92.

Wang Qianqian, and Qian Yongfu, 1997: Effects of diurnal variation of solar radiation on the simulated properties of the summer monsoon. *Acta Meteorlogica Sinica*, **55**, 334–345. (in Chinese)

Wang, Y. Q., O. L. Sen, and B. Wang, 2003: A highly resolved regional climate model (IPRC-RegCM) and its simulation of the 1998 severe precipitation event over China. Part I: Model description and verification of simulation. *J. Climate*, **16**, 1721–1738.

Webster, P. J., and S. Yang, 1992: Monsoon and ENSO: Selectively interactive systems. *Quart. J. Roy. Meteor. Soc.*, **118**, 877–926.

Wu Guoxiong, Liu Hui, Zhao Yucheng, and Li Weiping, 1996: A nine-layer atmospheric general circulation model and its performance. *Adv. Atmos. Sci.*, **13**, 1–18.

Wu Guoxiong, and Coauthors, 1997: Global ocean-atmosphere-land system model of LASG (GOALS/LASG) and its performance in simulation study. *Quart. J. Appl. Meteor.*, **8**(Suppl), 15–28. (in Chinese)

Wu, G. X., and Y. S. Zhang, 1998: Tibetan Plateau forcing and the timing of the monsoon onset over South Asia and the South China Sea. *Mon. Wea. Rev.*, **126**, 913–927.

Wu Guoxiong, and Liu Yiming, 2000: Thermal adaptation, overshooting, dispersion, and subtropical anticyclone. Part I: Thermal adaptation and overshooting. *J. Atmos. Sci.*, **24**, 433–446. (in Chinese)

Wu Tongwen, Liu Ping, Wang Zaizhi, Liu Yiming, Yu Rucong, and Wu Guoxiong, 2003: The performance of atmospheric component model R42L9 of GOALS/LASG. *Adv. Atmos. Sci.*, **20**, 726–742.

Xie , P., and P. A. Arkin, 1996: Analyses of global monthly precipitation using gauge observations, satellite estimates, and numerical model predictions. *J. Climate*, **9**, 840–858.

Xue, Y., P. J. Sellers, J. J. Kinter, and J. Shukla, 1991: A simplified biosphere model for global climate studies. *J. Climate*, **4**, 345–364.

Yang, S., and K. M. Lau, 1998: Influences of sea surface temperature and ground wetness on Asian summer monsoon. *J. Climate*, **11**, 3230–3246.

Yu Rucong, Li Wei, Zhang Xuehong, Liu Yiming, Yu Yongqiang, Liu Hailong, and Zhou Tianjun, 2000: Climate features related to eastern China summer rainfalls in the NCAR CCM3. *Adv. Atmos. Sci.*, **17**, 503–518.

Zhang Qiong, Wu Guoxiong, and Qian Yongfu, 2002: The bimodality of the 100hPa South Asia High and its relationship to the climate anomaly over East Asia in summer. *J. Meteor. Soc. Japan*, **80**, 733–744.

Zhang Xuehong, Shi Guangyu, Liu Hui, and Yu Yongqiang, 2000: *IAP Global Ocean-Atmosphere-Land System Model*, Science Press, Beijing, 252pp.

Zhu Qiangen, Wu Hong, and Xie Lian, 1987: The breakdown process and structure characteristics of the monsoon trough over Asia in summer. *J. Tropical Meteor.*, **1**, 1–8. (in Chinese)